

Effective Field Theory Power Counting at Finite Density

James V. Steele

*Center for Theoretical Physics and Laboratory for Nuclear Science
Massachusetts Institute of Technology, Cambridge, MA 02139, USA*
(November 9, 2000)

Abstract

Effective field theory is applied to finite-density systems with two-particle interactions exhibiting an unnaturally large scattering length, such as neutron matter. A new organizational scheme, identified for a large number of space-time dimensions, allows for convergent analytic calculations in many-body systems and is similar to the hole-line expansion of traditional nuclear physics.

PACS number(s): 21.65.+f, 24.10.Cn, 11.10.-z

Effective field theory (EFT) provides a way to systematically improve low-energy observables and make predictions for related processes. It has recently been applied to systems with an unnaturally large scattering length by adopting an organizational scheme that forces an infinite set of diagrams to be summed at leading order [1].

Extending the systematic language of an EFT to many-body systems would be beneficial for describing various systems of interest including nuclei, neutron stars, and atomic Fermi-Dirac condensates. Although sophisticated approximation techniques already exist for describing finite-density systems [2,3], error estimates are difficult to quantify and have been considered the “holy grail” of many-body physics by Brueckner.

At finite density, EFTs have given an accurate understanding of dilute systems [4] and of Fermi surface effects [5] such as the superconductor pairing gap [6,7]. Also, the Skyrme model and EFTs constructed at saturation density [8] can parameterize finite-density effects with only a few parameters. However, connecting bulk properties at finite density, such as the equation of state of nuclear matter (an idealized infinite system of protons and neutrons interacting only through the strong force), to known free-space interactions between the constituent particles requires a consistent organizational scheme (or power counting) at finite density. This will also allow many other interesting questions to be investigated, including whether nuclear matter binds in the chiral limit [9] and why nuclear matter saturates.

An EFT treatment of many-body systems automatically dictates the relevance of higher-particle contact interactions. For example, three-particle scattering composed of only two-body interactions has divergent loop corrections and the addition of an actual three-body contact interaction is required to regularize the result [10]. For nucleons in the triton, such a contact interaction has been shown to be as important as two-body interactions [11]. Therefore, it is natural to first focus on an EFT description of finite density systems with two states, such as neutron matter, since then Pauli’s exclusion principle requires three- and higher-body contact interactions to be multiplied by powers of momentum and the EFT implies these contributions are suppressed.

For neutrons, restricting the momenta to be below m_π and neglecting spin dependence will clarify the discussion since pions and other extended structure can be integrated out leaving only simple point-like interactions. In addition, the two proposed free-space EFT power countings, known as Λ -counting and Q -counting [1], yield equivalent results in this regime. Therefore, $\mathcal{O}(k_F/m_\pi)$ corrections will be implicit in the following. To make the relevant scales transparent, dimensional regularization with power divergence subtraction (PDS) [12] will be used below to regulate infinite integrals.

Non-relativistic particles with (spin-averaged) contact interactions are governed by the most general lagrangian

$$\begin{aligned} \mathcal{L}_{\text{eff}} = & N^\dagger \left(i\partial_t + \frac{\nabla^2}{2M} \right) N - C_0 (N^\dagger N)^2 + \frac{1}{2} C_2 \left[(N^\dagger \nabla N)^2 + ((\nabla N^\dagger) N)^2 \right] \\ & + C_2^p (N^\dagger \nabla N) \cdot ((\nabla N^\dagger) N) + \dots, \end{aligned} \quad (1)$$

with particle mass M , S -wave interactions C_0 and C_2 , P -wave interaction C_2^p , and higher derivatives and partial waves represented by the dots. Calculating observables using this non-renormalizable lagrangian leads to divergences which need to be regulated. One-loop scattering (Fig. 1a) with external relative momentum $\mathbf{k} = \frac{1}{2}(\mathbf{k}_1 - \mathbf{k}_2)$ in the PDS subtraction scheme is

$$\int \frac{d^3q}{(2\pi)^3} \frac{M}{k^2 - q^2 + i\epsilon} = -\frac{M}{4\pi}(\mu + ik). \quad (2)$$

This introduces the renormalization scale μ into amplitudes, and so the low-energy constants in Eq. (1) must also depend on μ to ensure observables are μ -independent.

Note that μ should be of the same order as the characteristic momentum of the process, k , so that the relative size of the loop Eq. (2) is not altered. Both scales should be small compared to the scale of underlying physics (m_π for neutrons) to ensure the EFT description does not break down. Furthermore, two-particle interactions exhibiting a large scattering length introduce a small momentum scale into the system (the neutron scattering length a_s gives $|1/a_s| \sim 10$ MeV). All this can be summarized by defining a generic small scale $Q \equiv (k, \mu, 1/a_s)$, and all observables are well approximated by an expansion in Q .

Matching the on-shell T-matrix to phase-shift data gives expressions for the low-energy constants of Eq. (1) in terms of scattering observables [12] such as the scattering length a_s and effective range r_e ,

$$C_0 = -\frac{4\pi/M}{\mu - 1/a_s} \sim \frac{1}{Q}, \quad C_2 k^2 = \frac{4\pi/M}{(\mu - 1/a_s)^2} \frac{r_e}{2} k^2 \sim Q^0.$$

Since the particle-particle loop Eq. (2) scales like Q , all insertions of C_0 contribute at leading order $1/Q$ to the T-matrix, whereas insertions of C_2 and other contact interactions are higher order. This justifies the Lippmann-Schwinger equation for C_0 only, which forms a summable geometric series, giving [12]

$$T(k) = \frac{C_0}{1 - \frac{MC_0}{4\pi}(\mu + ik)} = \frac{4\pi/M}{1/a_s + ik}. \quad (3)$$

Note that the result is μ -independent and produces the first term in the effective range expansion by construction.

A many-body system of fermions with spin-isospin degeneracy $g = (2S+1)(2I+1)$ forms a Fermi sea with Fermi momentum k_F and density $\rho = gk_F^3/6\pi^3$. The kinetic energy per particle of a free fermion gas is given by the familiar expression

$$\frac{E_{\text{kin}}}{A} = \frac{g}{\rho} \int \frac{d^3k}{(2\pi)^3} \frac{k^2}{2M} = \frac{3}{5} \frac{k_F^2}{2M}. \quad (4)$$

Quantum fluctuations allow particle-hole pairs to form, with interactions still given by the lagrangian Eq. (1). These contributions to the ground-state energy can be represented by closed, connected Feynman diagrams and calculated using finite-density Feynman rules [2,4].

Two basic building blocks of finite-density diagrams are depicted in Fig. 1a and b. Since the neutron propagator accounts for both particle and hole propagation

$$G_0(k)_{\alpha\beta} = \delta_{\alpha\beta} \left(\frac{\theta(k - k_F)}{k_0 - \mathbf{k}^2/2M + i\epsilon} + \frac{\theta(k_F - k)}{k_0 - \mathbf{k}^2/2M - i\epsilon} \right), \quad (5)$$

contour integration of the loop momentum shows Fig. 1a and b actually represent *three* processes: two-particle or two-hole scattering in Fig. 1a and one-particle, one-hole scattering in Fig. 1b. Pauli blocking is enforced by the following theta functions, which depend on

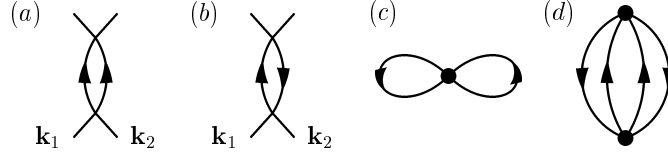


FIG. 1. Scattering with propagators in the same direction (a) and opposite directions (b). Also shown are the two simplest contributions to the ground-state energy (c) and (d).

the center of mass momentum $\mathbf{P} = \mathbf{k}_1 + \mathbf{k}_2$ and arbitrary relative momentum \mathbf{q} (with $\mathbf{q}_{1,2} = \frac{1}{2}\mathbf{P} \pm \mathbf{q}$),

$$\begin{aligned}\theta_q^+ &\equiv \theta(q_1 - k_F) \theta(q_2 - k_F) , \\ \theta_q^\pm &\equiv \theta(q_1 - k_F) \theta(k_F - q_2) , \\ \theta_q^- &\equiv \theta(k_F - q_1) \theta(k_F - q_2) ,\end{aligned}$$

for particle-particle, particle-hole, and hole-hole scattering respectively. These three processes can be integrated analytically:

$$\int \frac{d^3q}{(2\pi)^3} \frac{\theta_q^+}{k^2 - q^2 + i\epsilon} = -\frac{\mu}{4\pi} + \frac{k_F}{(2\pi)^2} f(\kappa, s) , \quad (6)$$

$$\int \frac{d^3q}{(2\pi)^3} \frac{\theta_q^\pm}{\mathbf{P} \cdot (\mathbf{k} - \mathbf{q}) + i\epsilon} = -\frac{k_F}{(2\pi)^2} \tilde{f}(\boldsymbol{\kappa} \cdot \mathbf{s}, s) , \quad (7)$$

$$\int \frac{d^3q}{(2\pi)^3} \frac{\theta_q^-}{q^2 - k^2 + i\epsilon} = \frac{k_F}{(2\pi)^2} f(\kappa, -s) \theta(1 - s) . \quad (8)$$

having defined the dimensionless momenta $\mathbf{s} = \frac{1}{2}\mathbf{P}/k_F$ and $\boldsymbol{\kappa} = \mathbf{k}/k_F$. Particle-particle scattering has contributions from momenta up to infinity and so can be written as a regularized integration over all momenta, Eq. (2), which brings the μ -dependence in Eq. (6), minus a term constraining at least one propagator to be inside the Fermi surface, which replaces the remnant of asymptotic scattering, ik , by the nontrivial function $f(\kappa, s)$. This same functional form appears in hole-hole scattering, but in this case both \mathbf{k}_1 and \mathbf{k}_2 must be inside the Fermi surface, and so $P < 2k_F$ (i.e. $s < 1$). In fact, the functions in Eqs. (6-8) have different analytical forms depending on whether $s > 1$ or $s < 1$, and the combinations which enter ground-state energy calculations are

$$\theta(1 - s) f(\kappa, s) = 1 + s + \kappa \ln \left| \frac{1 + s - \kappa}{1 + s + \kappa} \right| + \frac{1 - \kappa^2 - s^2}{2s} \ln \left| \frac{(1 + s)^2 - \kappa^2}{1 - \kappa^2 - s^2} \right| , \quad (9)$$

$$\theta(1 - s) \tilde{f}(\alpha s, s) = \frac{1 - \alpha}{2} + \alpha \ln \left| \frac{1 - s - \alpha}{\alpha} \right| + \frac{1 - (\alpha - s)^2}{4s} \ln \left| \frac{1 + s - \alpha}{1 - s - \alpha} \right| , \quad (10)$$

$$\theta(s - 1) \tilde{f}(\alpha s, s) = \frac{s - \alpha}{2s} + \frac{1 - (\alpha - s)^2}{4s} \ln \left| \frac{s + 1 - \alpha}{s - 1 - \alpha} \right| . \quad (11)$$

Interpreting one contribution to the ground-state energy, Fig. 1d, in three different ways gives the identities:

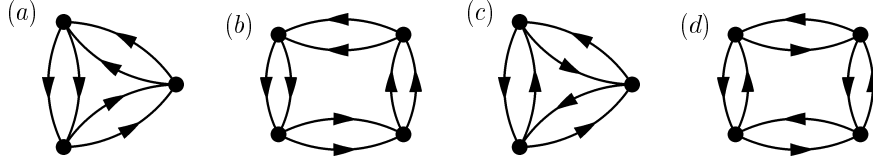


FIG. 2. Four representative contributions to the ground-state energy.

$$\begin{aligned}
& \int \frac{d^3k d^3P}{(2\pi)^6} \theta_k^- \left(f(\kappa, s) - \frac{\pi\mu}{k_F} \right) = - \int \frac{d^3k d^3P}{(2\pi)^6} \theta_k^- \tilde{f}(\boldsymbol{\kappa} \cdot \mathbf{s}, s) \\
& = \int \frac{d^3k d^3P}{(2\pi)^6} \theta_k^+ f(\kappa, -s) \theta(1-s) = \frac{k_F^6}{6\pi^4} \left(\frac{11 - 2 \ln 2}{35} - \frac{\pi\mu}{6k_F} \right), \quad (12)
\end{aligned}$$

which all integrate to the same result, serving as an excellent check of Eqs. (9-11).

Extending Q -counting to finite density shows the small parameter is $Q \equiv (k_F, \mu, 1/a_s)$, so all powers of $k_F a_s$ must be summed at leading order [13]. Also, this choice $\mu \sim k_F$ ensures the regularization does not destroy the relative importance of Eq. (6), since $f(\kappa, s)/\pi \sim \mathcal{O}(1)$. With this scaling, the kinetic energy per particle Eq. (4) is $\mathcal{O}(Q^2)$, and the contribution with one C_0 insertion, Fig. 1c, is

$$\left(\frac{E}{A} \right)_{(1c)} = \frac{g(g-1)}{2\rho} \int \frac{d^3k d^3P}{(2\pi)^6} \theta_k^- C_0 = \frac{(g-1)k_F^3}{12\pi^2} C_0 \sim Q^2. \quad (13)$$

The free-space counting $C_0 \sim 1/Q$ makes Eq. (13) of the same order as the kinetic energy and hence nontrivial properties such as nuclear binding can possibly occur at leading order. In fact, each additional C_0 vertex added to Fig. 1c requires two more propagators and one more loop integral, bringing an extra factor of order¹

$$C_0 \left(\frac{M}{k_F^2} \right)^2 \left(\frac{k_F^5}{M} \right) \sim Q^0 \quad (14)$$

and so *all* possible insertions of C_0 , including non-planar graphs, are leading order, making calculations intractable.

However, evaluation of some representative diagrams will show there is still an additional organizational scheme which can be exploited. Take, for example, the Feynman diagrams in Fig. 2a-d, which are all of the same order in Q -counting. They are rings of bubbles with particle scattering in either the same direction or opposite directions. A loop momentum is assigned to each bubble and a propagator Eq. (5) to each line. The final loop momentum can be chosen to be the center-of-mass momentum P , which traverses the entire ring and is shared equally by the legs of each bubble. A contour integration over the propagators enforces energy conservation, so not all propagators of a diagram can be particles (or holes).

¹The identification $k_0 \sim k^2/2M$ is made for power counting purposes [12].

The contributions to each diagram are: two particle-particle bubbles, one hole-hole bubble (2pp-1hh) and one particle-particle bubble, two hole-hole bubbles (1pp-2hh) for Fig. 2a; 3pp-1hh, 2pp-2hh, and 1pp-3hh for Fig. 2b; 2ph-1hp and 1ph-2hp for Fig. 2c; 3ph-1hp, 2ph-2hp, and 1ph-3hp for Fig. 2d. After working through the Feynman rules, simplifying the expressions, and dividing by the density ρ , the energy per particle for each diagram, organized according to the aforementioned particle and hole content, is:

$$\begin{aligned} \left(\frac{E}{A}\right)_{(2a)} &= (g-1) \frac{k_F^2}{2M} \left(\frac{Mk_F C_0}{4\pi}\right)^3 \frac{48}{\pi^3} \int \frac{d^3 s d^3 \kappa}{(4\pi)^2} \left[\theta_\kappa^- \left(f(\kappa, s) - \frac{\pi\mu}{k_F}\right)^2 + \theta_\kappa^+ f(\kappa, -s)^2 \right], \\ \left(\frac{E}{A}\right)_{(2b)} &= (g-1) \frac{k_F^2}{2M} \left(\frac{Mk_F C_0}{4\pi}\right)^4 \frac{48}{\pi^4} \int \frac{d^3 s d^3 \kappa}{(4\pi)^2} \\ &\quad \times \left[\theta_\kappa^- \left(f(\kappa, s) - \frac{\pi\mu}{k_F}\right)^3 + 3 \left(f(\kappa, s) - \frac{\pi\mu}{k_F}\right) \int \frac{d^3 q}{2\pi} \frac{\theta_\kappa^- \theta_q^+}{\kappa^2 - q^2} f(q, -s) + \theta_\kappa^+ f(\kappa, -s)^3 \right], \\ \left(\frac{E}{A}\right)_{(2c)} &= (g-1)(g-3) \frac{k_F^2}{2M} \left(\frac{Mk_F C_0}{4\pi}\right)^3 \frac{96}{2! \pi^3} \int \frac{d^3 s d^3 \kappa}{(4\pi)^2} \left[\theta_\kappa^\mp \tilde{f}(\boldsymbol{\kappa} \cdot \mathbf{s}, s)^2 + \theta_\kappa^\pm \tilde{f}(-\boldsymbol{\kappa} \cdot \mathbf{s}, s)^2 \right], \\ \left(\frac{E}{A}\right)_{(2d)} &= -(g-1)^2(g-3) \frac{k_F^2}{2M} \left(\frac{Mk_F C_0}{4\pi}\right)^4 \frac{96}{3! \pi^4} \int \frac{d^3 s d^3 \kappa}{(4\pi)^2} \\ &\quad \times \left[\theta_\kappa^\mp \tilde{f}(\boldsymbol{\kappa} \cdot \mathbf{s}, s)^3 - 3 \tilde{f}(\boldsymbol{\kappa} \cdot \mathbf{s}, s) \int \frac{d^3 q}{4\pi} \frac{\theta_\kappa^\mp \theta_q^\pm}{\mathbf{s} \cdot (\boldsymbol{\kappa} - \mathbf{q})} \tilde{f}(-\mathbf{q} \cdot \mathbf{s}, s) + \theta_\kappa^\pm \tilde{f}(-\boldsymbol{\kappa} \cdot \mathbf{s}, s)^3 \right], \end{aligned}$$

where a factor of $\theta(1-s)$ has been absorbed into $f(\kappa, -s)$. The factor of “3” in contributions to Fig. 2b and d comes from the combinatorics of choosing the second pp or ph pair respectively and the symmetry factor of Fig. 2d gives an additional 1/3 suppression compared to the other diagrams.

A simple change of variables shows the i ph- j hp and j ph- i hp contributions are the same for any i and j . Numerically integrating the above expressions and taking $\mu = 0$ for clarity gives

$$\left(\frac{E}{A}\right)_{(2a)} = (g-1) \frac{k_F^2}{2M} (k_F a_s)^3 (0.0641 + 0.0115), \quad (15)$$

$$\left(\frac{E}{A}\right)_{(2b)} = (g-1) \frac{k_F^2}{2M} (k_F a_s)^4 (0.0383 + 3 \times 0.00247 - 0.000683), \quad (16)$$

$$\left(\frac{E}{A}\right)_{(2c)} = (g-1)(g-3) \frac{k_F^2}{2M} (k_F a_s)^3 (0.0287 + 0.0287), \quad (17)$$

$$\left(\frac{E}{A}\right)_{(2d)} = -(g-1)^2(g-3) \frac{k_F^2}{2M} (k_F a_s)^4 (0.000603 + 3 \times 0.000557 + 0.000603). \quad (18)$$

Adding the terms for each of the three-bubble diagrams, Fig. 2a and c, gives results in agreement with Ref. [4]. Comparison of individual terms in Eqs. (15-18) shows each additional hole-line is suppressed by about a factor of three. This means every added hole-hole bubble is suppressed by almost an order of magnitude. The suppression is the same at nonzero μ , where $k_F a_s$ can be taken very large.

This suppression can be described by a new power counting at finite density which is kinematical in nature and will lead to the simplification of many-body calculations. Take

the 1pp-1hh contribution of Eq. (12), which using Eq. (6) can be written in terms of one relative momentum below the Fermi surface and another above:

$$\int \frac{d^3 P d^3 k d^3 q}{(2\pi)^9} \frac{\theta_k^- \theta_q^+}{k^2 - q^2 + i\epsilon} = \int \frac{d^3 P d^3 k d^3 q}{(2\pi)^9} \frac{\theta_k^- \theta_q^+}{-q^2 + i\epsilon} \left(1 - \frac{k^2}{-q^2 + i\epsilon} + \mathcal{O}(k^4/q^4) \right). \quad (19)$$

The integration region θ_k^- can be pictured as the overlap of two Fermi spheres (of radius k_F) with centers separated by the center-of-mass momentum \mathbf{P} , whereas the region θ_q^+ is given by all momenta excluding these same intersecting spheres [2]. In principle, the momenta k and q can both be near k_F , but the integration measure $d^3 P$ suppresses $P \sim 0$, which makes the approximation $q \gg k$ appropriate.

In addition, for $P \lesssim 2k_F$, the overlap region of the two spheres is small and suppresses additional powers of k^2 in the numerator, since

$$\int \frac{d^3 \kappa}{4\pi} \frac{\theta_\kappa^+}{-\kappa^2 + i\epsilon} = -\frac{\pi\mu}{2k_F} + 1 + \mathcal{O}(1-s), \quad (20)$$

$$\int \frac{d^3 \kappa}{4\pi} \theta_\kappa^- = \frac{(1-s)^2}{2} + \mathcal{O}(1-s)^3, \quad (21)$$

and more generally $\theta_q^+/q^{2n} \sim \mathcal{O}(1-s)^0$ for every n , and $\theta_k^- k^{2n} \sim \mathcal{O}(1-s)^{n+2}$. Then, working in D dimensions (with the understanding that $D = 4$ will be taken at the end of the calculation) the integral over the center-of-mass momentum gives

$$\int_0^1 ds s^{D-2} (1-s)^n \sim \frac{1}{D^n} \int_0^1 ds s^{D-2}. \quad (22)$$

for large D . In fact, carrying out the entire calculation in D -dimensions shows the suppression is actually $1/\mathcal{D}^n$ with $\mathcal{D} \equiv 2^{D/2}$, which is numerically equivalent to Eq. (22) for $D = 4$ but even more convergent in larger number of dimensions.

From the above, the theta functions which enforce Pauli blocking can be associated with powers of $1/\mathcal{D}$: $\theta_\kappa^+ \sim 1/\mathcal{D}^0$, $\theta_\kappa^- \sim 1/\mathcal{D}^2$, and Eq. (12) implies $\theta_\kappa^\pm \sim 1/\mathcal{D}$. Therefore, the expansion in $1/\mathcal{D}$ is similar to the traditional hole-line expansion of nuclear physics [2]. Furthermore, the complicated functions of Eq. (9-11) greatly simplify to

$$f(\kappa, s) = 2 + \mathcal{O}(\mathcal{D}^{-1}), \quad f(\kappa, -s) = -\frac{(1-s)^2}{\kappa^2} + \mathcal{O}(\mathcal{D}^{-3}), \quad (23)$$

since they always appear with the respective theta functions θ_κ^- and θ_κ^+ , and using Eq. (12),

$$\theta(s-1) \tilde{f}(\alpha s, s) = \frac{1}{3s(s-\alpha)} + \mathcal{O}(\mathcal{D}^{-2}). \quad (24)$$

Using these simplified forms along with Eqs. (20-21), the above analytic expressions for the diagrams of Fig. 2 can be analytically integrated. The numerical values at each order in $1/\mathcal{D}$ are collected in Table I, and the $1/\mathcal{D}$ -expansion quickly converges to the full result in most cases, although the contributions to Fig. 2c require further investigation.

The existence of a power counting in $1/\mathcal{D}$ allows for systematic calculation of finite-density observables such as the ground-state energy. First of all, it is interesting to note that at next-to-leading order in the Q -expansion, one insertion of $C_2 k^2$ will appear, and the

TABLE I. Exact factors in contributions to the energy per particle of Eq. (15-18) and their respective expansion in powers of $1/\mathcal{D}$. An overall factor of “3” for the 2pp-2hh and 2ph-2hp terms has been left out below for a more direct comparison. The 1pp-3hh diagram first appears at order $1/\mathcal{D}^6$ with contribution -0.000507 .

	Fig. 2a		Fig. 2b			Fig. 2c	Fig. 2d	
	2pp-1hh	1pp-2hh	3pp-1hh	2pp-2hh	1pp-3hh	2ph-1hp	3ph-1hp	2ph-2hp
total	0.0641	0.0115	0.0383	0.00247	-0.000683	0.0287	0.000603	0.000557
$\mathcal{O}(1/\mathcal{D}^2)$	0.0860	—	0.0548	—	—	—	—	—
$\mathcal{O}(1/\mathcal{D}^3)$	-0.0162	—	-0.0155	—	—	0.0283	—	—
$\mathcal{O}(1/\mathcal{D}^4)$	-0.0056	0.0133	-0.0032	0.00310	—	0.0057	0.000676	0.000676
$\mathcal{O}(1/\mathcal{D}^5)$	0.0002	-0.0024	-0.0007	-0.00164	—	-0.0003	0.000371	-0.000230

integration of k^2 over phase space (θ_k^-) brings a factor of $1/\mathcal{D}$. Therefore the hierarchy of the Q -expansion is already included in the $1/\mathcal{D}$ -expansion. The leading order ground-state energy per particle can be written in closed form:

$$\frac{E}{A} = \frac{E_{\text{kin}}}{A} + \frac{E_{\text{int}}^{(0)}}{A} + \mathcal{O}(1/\mathcal{D}), \quad (25)$$

with the kinetic energy given by Eq. (4) and the interaction energy to this order given by all the particle-particle scattering terms (i.e., the n pp-1hh bubbles for all n). This is a summable geometric series, giving

$$\frac{E_{\text{int}}^{(0)}}{A} = \frac{g(g-1)}{2\rho} \int \frac{d^3P d^3k}{(2\pi)^6} \theta_k^- \frac{4\pi/M}{1/a_s - \frac{k_E}{\pi} f(\kappa, s)}, \quad (26)$$

which is μ -independent, as it should be for any consistent expansion. Actually, to the order quoted in $1/\mathcal{D}$, the substitution $f(\kappa, s) \rightarrow 2$ is valid, which gives the leading-order ground-state energy per particle for neutron matter (taking $g = 2$)

$$\frac{E}{A} = \left(\frac{3}{5} + \frac{2k_F a_s/3}{\pi - 2k_F a_s} \right) \frac{k_F^2}{2M} + \mathcal{O}(1/\mathcal{D}). \quad (27)$$

For $a_s > 0$, E/A has a pole at $k_F a_s = \pi/2$ and it would be interesting to explore its consequence in atomic systems where the scattering length can be tuned. As for neutrons, the scattering length is negative and it is a good approximation to take $1/a_s \rightarrow 0$, to arrive at the scale-invariant answer $E/A = (4/15)k_F^2/2M$. The next order in $1/\mathcal{D}$ will require a single insertion of C_2 or C_2^p and diagrams with three hole-lines.

A new power counting at finite density has been found which includes the nonperturbative free-space power counting of two-nucleon EFTs. The many-body problem simplifies in a large number of space-time dimensions and leads to a convergent expansion even for $D = 4$. Including explicit pions and three-body forces in the lagrangian will allow the above analysis to be extended to nuclear matter for an exploration of the behavior near saturation density.

I would like to thank R. J. Furnstahl, H. W. Hammer, D. B. Kaplan, J. W. Negele, and K. Rajagopal for useful discussions and I. W. Stewart for a critical reading of the manuscript. This work was supported in part by the U.S. Department of Energy under cooperative research agreement #DF-FC02-94ER40818.

REFERENCES

- [1] S. Weinberg, Nucl. Phys. **B363**, 3 (1991);
Proceedings of the Joint Caltech/INT Workshop: *Nuclear Physics with Effective Field Theory*, ed. R. Seki, U. van Kolck, and M.J. Savage (World Scientific, 1998).
- [2] A. L. Fetter and J. D. Walecka, *Quantum Theory of Many-Particle Systems* (McGraw-Hill, New York, 1971);
J. W. Negele and H. Orland, *Quantum Many-Particles Systems* (Addison-Wesley, New York, 1988).
- [3] K. A. Brueckner, *The Many Body Problem*, edited by C. DeWitt (John Wiley and Sons, New York, 1959), p. 47;
H. A. Bethe, Ann. Rev. Nucl. Sci. **21**, 93 (1971);
B. D. Day, Rev. Mod. Phys. **39**, 719 (1967); *ibid* **50**, 495 (1978);
V. R. Pandharipande and R. B. Wiringa, *ibid* **51**, 821 (1979).
- [4] H. W. Hammer and R. J. Furnstahl, Nucl. Phys. **A678**, 277 (2000).
- [5] R. Shankar, Physica **A177**, 530 (1991); Rev. Mod. Phys. **66**, 129 (1994);
J. Polchinski, hep-th/9210046.
- [6] T. Papenbrock and G. F. Bertsch, Phys. Rev. **C59**, 2052 (1999).
- [7] N. Evans, S. D. Hsu and M. Schwetz, Nucl. Phys. **B551**, 275 (1999);
T. Schafer and F. Wilczek, Phys. Lett. **B450**, 325 (1999).
- [8] M. Lutz, B. Friman and C. Appel, Phys. Lett. **B474**, 7 (2000);
M. Lutz, Nucl. Phys. **A670**, 214 (2000);
B. Krippa, hep-ph/0006305.
- [9] A. Bulgac, G. A. Miller and M. Strikman, Phys. Rev. **C56**, 3307 (1997).
- [10] E. Braaten and A. Nieto, Phys. Rev. **B55**, 8090 (1997); *ibid* **56**, 14745 (1997).
- [11] P. F. Bedaque, H. W. Hammer and U. van Kolck, Nucl. Phys. **A676**, 357 (2000).
- [12] D. B. Kaplan, M. J. Savage and M. B. Wise, Nucl. Phys. **B534**, 329 (1998).
- [13] R. J. Furnstahl, J. V. Steele and N. Tirfessa, Nucl. Phys. **A671**, 396 (2000).